

Coexisting sonographic features of “tumor neovascularization-like pattern” and “echogenic areas” in thyroid nodules: diagnostic performance in prediction of papillary carcinoma

Meng-Ying Tong¹, Meng Qiu², Xiao Feng¹, Li-Ying Guo¹, Wen-Long Xie¹, Juan-Juan Jia³, Ying Che¹

¹Department of Ultrasound, The First Affiliated Hospital of Dalian Medical University, Dalian, Liaoning 116044, China;

²Graduate Institute of Dalian Medical University, Dalian, Liaoning 116044, China;

³Department of Pathology, The First Affiliated Hospital of Dalian Medical University, Dalian, Liaoning 116044, China.

To the Editor: Many well-studied sonographic features have been used clinically to evaluate thyroid nodules for malignancies. Sonographic grayscale features proposed by the American College of Radiology Thyroid Imaging, Reporting and Data System (TI-RADS) include composition, echogenicity, shape, margin, and echogenic foci.^[1] Other features, such as vascularity imaging, have gradually been recognized by sonographers. Sustained angiogenesis results in tumor-specific vasculature compared to normal tissues in the context of architecture and biological behavior.^[2] Tumor neovascularization shows abnormal maturation, manifesting irregular sprouting, and branching of angiogenic vessels with disordered coverage of pericytes. Therefore, vascularity is critical for the evaluation of malignancy in thyroid nodules.

Color Doppler flow imaging (CDFI) is theoretical to classify malignancy on the basis of vascular information. However, existing studies have not reached an agreement regarding its assessment. One of the reasons is that the previous studies simply took the abundance and distribution of vascular flow into consideration, regardless of vascular architecture.^[3] Here, we have found that nodules with intense small penetrating vessels on CDFI, termed tumor neovascularization-like pattern (TNLP), are often associated with papillary thyroid cancers (PTC). Moreover, we have observed a correlation and coexistence of TNLP and echogenic areas (EA) on ultrasound, which may be a helpful sonographic finding that could increase suspicion for malignancy.

Standard institutional board review approval was obtained from the First Affiliated Hospital of Dalian Medical University (No. YJ-KY-2020-50). The patients were contacted by telephone to obtain verbal informed

consent for the tissue slides used in this study. Between June 2018 and October 2018, a total of 215 patients underwent ultrasound-guided fine-needle aspiration (FNA) of the thyroid and had clear cytological diagnosis, complete clinical information, and ultrasonic images [Supplementary Table 1, <http://links.lww.com/CM9/A310>]. These patients had 299 nodules, with 161 PTCs and 138 benign nodules. Detailed materials and methods of patient cohort [Supplementary Figure 1, <http://links.lww.com/CM9/A310>], collection and evaluation of ultrasound images, tissue samples, scoring system, and statistical analysis are provided in Supplementary File, <http://links.lww.com/CM9/A311>.

Nodular microvascular flow was evaluated with CDFI in the 299 nodules. In terms of the merging methods recommended by Shin *et al*,^[4] Chen *et al*,^[5] and our experience, nodular vascularity on CDFI was classified into four types [Figure 1A]: type I, absence of nodule vascularity; type II, predominantly perinodular vascularity with continuous (IIa) or discontinuous circumferential vascularity at the margin of a nodule (IIb); type III, predominantly intranodular vascularity, homogenous linear (IIIa) or branching (IIIb) with or without perinodular vascularity; type IV, heterogeneous short-line, strip-like, or microbubble colorful signals, which penetrated the margin of the nodule (perinodular neovascularization, IVa) or dispersedly distributed within the nodule (internal neovascularization, IVb). TNLP, identified as vascularity of type IV, was more commonly found in malignant nodules, which had a sensitivity of 45.3% and a specificity of 90.6%. The presence of TNLP increased the risk of PTC by an odds ratio of 7.976 (95% confidence interval [CI], 4.164–15.279, $P < 0.0001$) [Supplementary Tables 2 and 3, <http://links.lww.com/CM9/A310>].

Meng-Ying Tong and Meng Qiu contributed equally to this work.

Correspondence to: Ying Che, Department of Ultrasound, The First Affiliated Hospital of Dalian Medical University, Dalian, Liaoning 116044, China
E-Mail: cheying@dmu.edu.cn

Copyright © 2020 The Chinese Medical Association, produced by Wolters Kluwer, Inc. under the CC-BY-NC-ND license. This is an open access article distributed under the terms of the Creative Commons Attribution-Non Commercial-No Derivatives License 4.0 (CCBY-NC-ND), where it is permissible to download and share the work provided it is properly cited. The work cannot be changed in any way or used commercially without permission from the journal.

Chinese Medical Journal 2020;133(21)

Received: 03-03-2020 Edited by: Li-Shao Guo

Access this article online

Quick Response Code:



Website:

www.cmj.org

DOI:

10.1097/CM9.0000000000001077

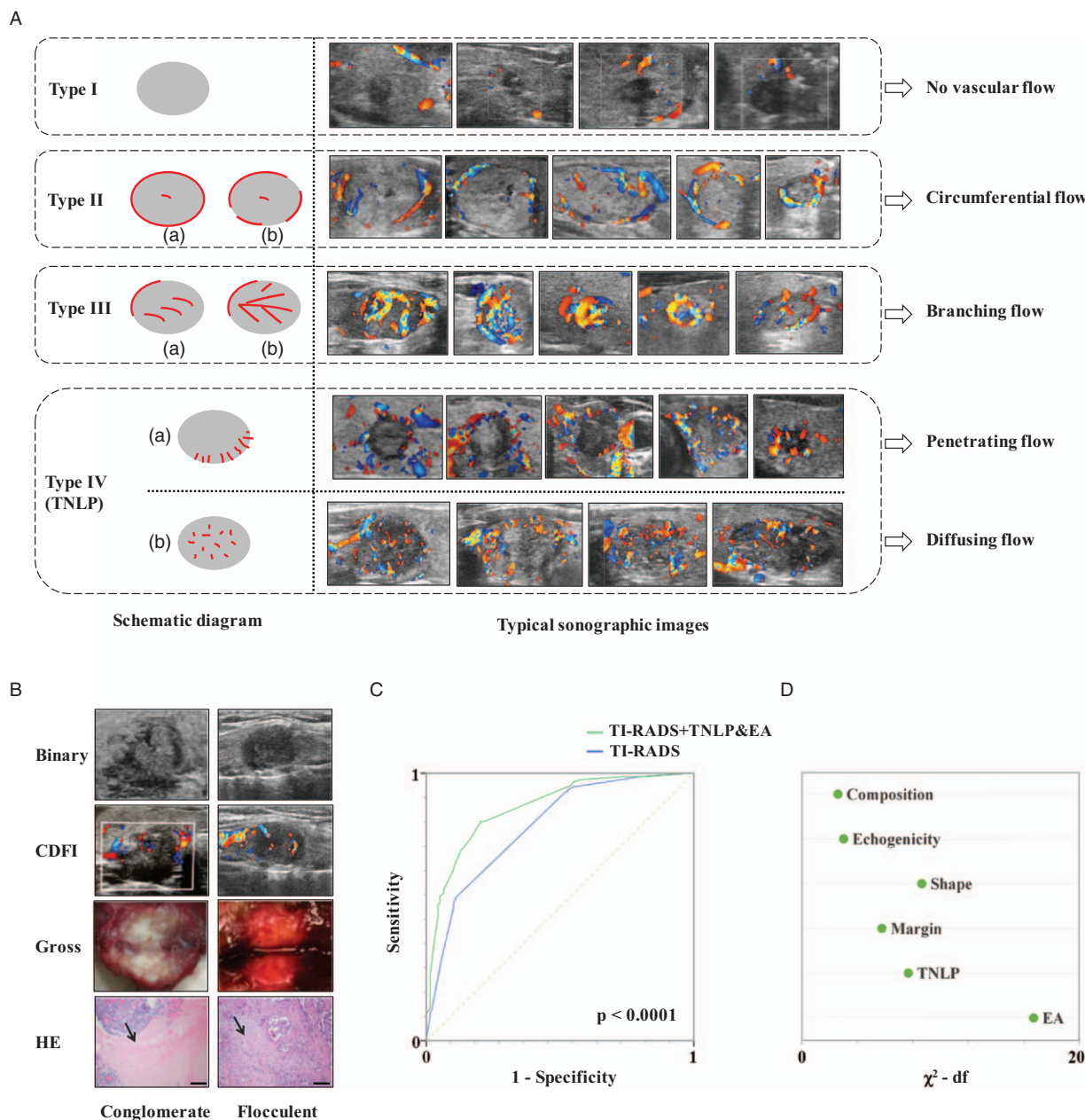


Figure 1: Illustration and role of TNLP and EA in thyroid nodules. (A) Schematic diagram and sonographic images illustrating the CDFI vascularity types of thyroid nodules. Type I: absence of nodule vascularity. Type II: predominantly perinodular vascularity with continuous (IIa) or discontinuous circumferential (IIb) vascularity at the margin of a nodule. Type III: predominantly intranodular vascularity, linear (IIIa) or branching (IIIb). Type IV (TNLP): penetrating (perinodular neovascularization, IVa) or diffusing (internal neovascularization, IVb) vascularity of a nodule. (B) Representative conglomerate and flocculent fibrotic EA in the individual cases of PTCs. Sonographic image of binary manner (top) and CDFI (2nd), cut surface of the resected nodule (3th) and HE staining (bottom). Scale bars indicate 200 μ m. The arrows indicate fibrosis. (C) Receiver operating characteristic (ROC) curves for prediction of malignancy, using logistic regression models that include composition, echogenicity, shape, margin and echogenic foci as covariates, with (green line) or without (blue line) TNLP and EA. (D) Significance (Chi-squared statistic) of each covariate for prediction of malignancy in the multivariate model that includes TNLP and EA. CDFI: Color Doppler flow imaging; df: Degrees of freedom; EA: Echogenic areas; HE: Hematoxylin-eosin; PTC: Papillary thyroid cancers; TNLP: Tumor neovascularization-like pattern.

The feature of EA on ultrasound was evaluated in a binary manner. EA were defined as homogeneous mild hyperechoic areas (excluding microcalcifications) located within the relatively hypoechoic nodule. The morphology of EA was either conglomerate or flocculent [Figure 1B]. Based on our interpretations, the feature had a sensitivity of 59.0% and a specificity of 91.3%. The presence of EA increased the risk of PTC by an odds ratio of 15.114 (95% CI, 7.732–29.543, $P < 0.0001$) [Supplementary Tables 2 and 3, <http://links.lww.com/CM9/A310>]. Additionally, we

found a significant correlation between TNLP and EA on ultrasound in the malignant nodules ($r = 0.430$, $P < 0.0001$). The distribution of the two features within one nodule was not overlapped. Flocculent EA often existed in the nodules with internal neovascularization [Figure 1A, Type IVb], manifested as the microvascular signals and flocculent EA dispersed within the nodules. Conglomerate EA often existed in the center of the nodules with perinodular neovascularization [Figure 1A, Type IVa].

To investigate the pathological basis of EA on binary, a total of ten malignant nodules found to have EA on binary were randomly selected for pathological specimen review, demonstrating extensive fibrosis. Moreover, we found the pathologic correlation of the tumor neovascularization and fibrosis in malignant nodules. In the nodules with perinodular neovascularization, few viable cells and microvascular vessels were located in the regions of central EA, as the tissue had been almost entirely replaced by conglomerate fibrosis. In the nodules with internal neovascularization, intranodular flocculent fibrosis was surrounded by tumor cells and microvascular networks [Figure 1B].

We next tested the ability of the two features to predict the malignancy of nodules. The newly identified features as a single variable were more predictive of malignancy than the well-studied features recommended by TI-RADS, which include solidness, hypoechogenicity, taller-than-wide shape, extrathyroidal extended margin and presence of punctate echogenic foci [Supplementary Tables 2 and 3, <http://links.lww.com/CM9/A310>]. In multivariate logistic regression models that also considered composition, echogenicity, shape, margin and echogenic foci, inclusion of the newly identified features markedly improved predictive ability (Figure 1C; the area under the receiver operator characteristic curve = 0.873 *vs.* 0.801, $P < 0.0001$), and the presence of EA was the most significant covariate as measured by the Wald Chi-squared statistic [Figure 1D]. These results demonstrate that the newly identified features improve the ability to predict the malignancy of nodules.

The lack of vascularity has traditionally been considered to be suggestive of PTC, possibly because extensive fibrosis frequently exists in PTCs. Sonographers have frequently overlooked the vascular architecture observed with CDFI. We have skipped the ideological restraints and found that a specific vascular architecture was significantly associated with PTCs. Moreover, the TNLP was not excluded from fibrotic EA. These features frequently coexisted in PTCs on ultrasound, leading to elevated specificity in diagnosing PTCs. Although the newly identified features had high specificity, the sensitivity was relatively lower. Thus, vascularity and EA alone were insufficient for determination of PTCs. We then brought suspicious grayscale features, TNLP

and EA into a multivariate regression analysis. The results showed that inclusion of the new features markedly improved predictive ability, indicating combination of the new and conventional features may become the choice for differentiating PTCs from benign nodules. Therefore, when we make the decision of whether to conduct FNA with regard to the indeterminate nodules on ultrasound, especially for the solid and hypoechoic nodules without any other suspicious features, the newly identified features can potentially serve to influence the management decisions.

Funding

This work was supported by a grant from the Natural Science Foundation of Liaoning Province (No. 201602221).

Conflicts of interest

None.

References

1. Tessler FN, Middleton WD, Grant EG, Hoang JK, Berland LL, Teefey SA, *et al.* ACR thyroid imaging, reporting and data system (TI-RADS): white paper of the ACR TI-RADS committee. *J Am Coll Radiol* 2017;14:587–595. doi: 10.1016/j.jacr.2017.01.046.
2. Rajabi S, Dehghan MH, Dastmalchi R, Jalali Mashayekhi F, Salami S, Hedayati M. The roles and role-players in thyroid cancer angiogenesis. *Endocr J* 2019;66:277–293. doi: 10.1507/endocrj.EJ18-0537.
3. Liang XW, Cai YY, Yu JS, Liao JY, Chen ZY. Update on thyroid ultrasound: a narrative review from diagnostic criteria to artificial intelligence techniques. *Chin Med J* 2019;132:1974–1982. doi: 10.1097/CM9.0000000000000346.
4. Shin JH, Baek JH, Chung J, Ha EJ, Kim JH, Lee YH, *et al.* Ultrasonography diagnosis and imaging-based management of thyroid nodules: revised Korean society of thyroid radiology consensus statement and recommendations. *Korean J Radiol* 2016;17:370–395. doi: 10.3348/kjr.2016.17.3.370.
5. Chen L, Zhan J, Diao XH, Liu YC, Shi YX, Chen Y, *et al.* Additional value of superb microvascular imaging for thyroid nodule classification with the thyroid imaging reporting and data system. *Ultrasound Med Biol* 2019;45:2040–2048. doi: 10.1016/j.ultrasmedbio.2019.05.001.

How to cite this article: Tong MY, Qiu M, Feng X, Guo LY, Xie WL, Jia JJ, Che Y. Coexisting sonographic features of “tumor neovascularization-like pattern” and “echogenic areas” in thyroid nodules: diagnostic performance in prediction of papillary carcinoma. *Chin Med J* 2020;133:2638–2640. doi: 10.1097/CM9.0000000000001077